Journal of Microbiology (2023) 61:211–220
https://doi.org/10.1007/s12275-023-00013-z

MICROBIAL GENETICS, GENOMICS AND MOLECULAR BIOLOGY

# Relaxed Cleavage Specificity of Hyperactive Variants of *Escherichia coli* RNase E on RNA I

**Dayeong Bae[1] · Hana Hyeon[1] · Eunkyoung Shin[1] · Ji-Hyun Yeom[1] · Kangseok Lee[1]**

Received: 20 December 2022 / Revised: 26 December 2022 / Accepted: 27 December 2022 / Published online: 22 February 2023


## Abstract

RNase E is an essential enzyme in *Escherichia coli*. The cleavage site of this single-stranded specific endoribonuclease is well-characterized in many RNA substrates. Here, we report that the upregulation of RNase E cleavage activity by a mutation that affects either RNA binding (Q36R) or enzyme multimerization (E429G) was accompanied by relaxed cleavage specificity. Both mutations led to enhanced RNase E cleavage in RNA I, an antisense RNA of ColE1-type plasmid replication, at a major site and other cryptic sites. Expression of a truncated RNA I with a major RNase E cleavage site deletion at the 5′-end (RNA $I_{-5}$) resulted in an approximately twofold increase in the steady-state levels of RNA $I_{-5}$ and the copy number of ColE1-type plasmid in *E. coli* cells expressing wild-type or variant RNase E compared to those expressing RNA I. These results indicate that RNA $I_{-5}$ does not efficiently function as an antisense RNA despite having a triphosphate group at the 5′-end, which protects the RNA from ribonuclease attack. Our study suggests that increased cleavage rates of RNase E lead to relaxed cleavage specificity on RNA I and the inability of the cleavage product of RNA I as an antisense regulator in vivo does not stem from its instability by having 5′-monophosphorylated end.

**Keywords** RNase E · RNA I · Plasmid copy number · Cleavage specificity · Endoribonuclease

## Introduction

RNase E (Rne), encoded by *rne*, is an essential endoribonuclease for the degradation and processing of RNAs in *Escherichia coli* (Cohen, 1995; Gao et al., 2006; Ghora & Apirion, 1978; Hagege & Cohen, 1997; Jain & Belasco, 1995; Lee & Cohen, 2003; Lee et al., 2002, 2021a, 2021b, 2021c; Li & Deutscher, 2002;). RNase E initiates the degradation of a large portion of mRNA and processes various precursor RNAs, such as tRNA, 16S rRNA, and M1 RNA (Gurevitz & Apirion, 1983; Gurevitz et al., 1983; Kim et al., 1996; Li et al., 1999). RNase E can also regulate ColE1-type plasmid replication by cleaving RNA I, an antisense RNA (Lin-Chao & Cohen, 1991; Lin-Chao et al., 1994). RNase E preferentially cleaves the AU-rich region of single-stranded RNA and generates 3′-hydroxylated and 5′-monophosphorylated cleavage products (Arraiano et al., 2010; Huang et al., 1998; McDowall et al., 1994). In addition, RNase E cleavage of RNA substrates can potentially be affected by the state of 5′-phosphorylation (Feng et al., 2002; Jiang & Belasco, 2004; Mackie, 1998), secondary structure E (Bandyra et al., 2018; Richards & Belasco, 2021; Updegrove et al., 2019), and differences in the affinity of the enzyme for target sites with different sequences (Lin-Chao et al., 1994; McDowall et al., 1994).

RNase E (118 kDa) contains 1061 amino acids and can be separated into two halves. The N-terminal half (NTH-Rne: residues 1–529) of RNase E exhibits a catalytic function and cleavage site specificity and is essential for cell survival (Kido et al., 1996; McDowall & Cohen, 1996; McDowall et al., 1995). X-ray crystallography of NTH-Rne revealed six subregions: the RNase H domain, S1 domain, 5′-sensor, Dnase I domain, Zn-link domain, and small domains (Callaghan et al., 2005). The ribonucleolytic activity and expression levels of Rnase E are tightly controlled in *E. coli*. The depletion, adventitious overexpression, or increased enzymatic activity of Rnase E causes growth retardation of cells

Dayeong Bae and Hana Hyeon contributed equally to this work.

✉ Ji-Hyun Yeom
jihyun82@cau.ac.kr

✉ Kangseok Lee
kangseok@cau.ac.kr

[1] Department of Life Science, Chung-Ang University, Seoul 06974, Republic of Korea

(Go et al., 2011; Lee & Cohen, 2003; Moore et al., 2021; Shin et al., 2008). The autoregulatory mechanism ensures the stable expression level of RNase E in vivo through such that the enzyme cleaves its own mRNA (Jain & Belasco, 1995). In addition, the endonucleolytic activity of RNase E is controlled by several trans-acting factors (Gao et al., 2006; Lee & Cohen, 2003; Lee et al., 2021a, 2021b, 2021c; Moore et al., 2021; Singh et al., 2009). Recent studies indicate that homologs of RraA, one of these trans-acting regulators, play roles in the pathogenicity of *Salmonella Typhimurium* and *Vibrio vulnificus* via modulation of RNase E activity (Lee et al., 2021a, 2021b, 2021c, 2022).

Previous studies have isolated loss-of-function or hyperactive variants of RNase E using a genetic screening method (Go et al., 2011; Moore et al., 2021; Shin et al., 2008). These studies have identified and characterized two hyperactive RNase E variants. Q36R, which replaces glutamine with arginine at position 36 in the S1 domain, is a hyperactive mutation. RNase E activity was enhanced via reduced noncompetitive inhibition of the RNA substrate bound to the $^{24}$LYDLDIESPGHEQK$^{37}$ peptide region (Go et al., 2011). Another hyperactive RNase E mutation (E429G), in which glutamic acid is substituted with glycine at position 429, is located close to the Zn-link domain and contributes to the enhanced multimer formation of RNase E (Moore et al., 2021). Increased multimerization improves the ribonucleolytic activity of the enzyme on longer substrates, but not the cleavage of shorter oligomers that contain the same cleavage sequence (Moore et al., 2021).

Many RNA substrates of this single-stranded specific endoribonuclease are well-characterized. Among them, RNase E cleaves five nucleotides from the 5′-ends of RNA I, and the intermediates (RNA $I_{-5}$) are rapidly degraded by exonucleases, such as poly (A) polymerase or PNPase (Cohen, 1995; Xu et al., 1993). RNA $I_{-5}$ barely binds to RNA II in vitro, leading to the loss-of-function of RNA I as an antisense regulator (Tamm & Polisky, 1985; Tomizawa, 1984). In this study, we investigated the enzymatic properties of RNase E mutations that lead to hyperactivity of the enzyme (Rne-Q36R and Rne-E429G) on the cleavage of RNA I and its intermediate RNA $I_{-5}$.

## Materials and Methods

### Bacterial Strains, Plasmids, and Oligonucleotides

All strains, plasmids, and oligonucleotides used in this study are listed in Tables 1 and 2. KSL2000 (Rne-WT, Rne-Q36R, and Rne-E429G) strains were grown at 37 °C in Luria–Bertani (LB) broth (Becton, Dickinson and Company) supplemented with 0.1% L-arabinose (Sigma–Aldrich). The antibiotics were prepared at the following concentrations: 100 μg/ml kanamycin, 5 μg/ml tetracycline, and 5 μg/ml chloramphenicol. To construct pET3a expressing a variant of RNA I with a major RNase E cleavage site deletion at the 5′-end, RNA I with five nucleotides deleted from the 5′-end was amplified using the primers RNA I-5del (F), RNA I-5del-M (R), RNA I-5del-M (F), and RNA I-5del (R). Amplified polymerase chain reaction products were digested with PstI and AflIII and ligated into pET3a using T4 DNA ligase (Enzynomics).

### Growth Curve

Growth curves were measured as described previously (Lee et al., 2021a, 2021b, 2021c). Briefly, pre-cultured KSL2000-derived strains were diluted 100-fold with LB medium supplemented with 0.1% L-arabinose, 100 μg/ml kanamycin, 5 μg/ml tetracycline, and 5 μg/ml chloramphenicol, and

**Table 1** List of strains and plasmids used in this study

| | Description | References |
|---|---|---|
| *Strains* | | |
| N3433 | *lacZ43*(Fs) LAM$^-$ *relA1 spoT1 thi-1* | Goldblum and Apririon (1981) |
| KSL2000 | Same as N3433 but *rne::cat recA::Tn10* [pBAD-RNE] | Lee et al. (2002) |
| KSL2000-Q36R | Same as KSL2000 but [pBAD-RNE-Q36R] | This study |
| KSL2000-E429G | Same as KSL2000 but [pBAD-RNE-E429G] | This study |
| *Plasmids* | | |
| pBAD-RNE | pSC101 *ori*, Km$^r$, wild-type *rne* under $P_{BAD}$ | Lee et al. (2002) |
| pBAD-RNE-Q36R | pSC101 *ori*, Km$^r$, *rne*-Q36R under $P_{BAD}$ | This study |
| pBAD-RNE-E429G | pSC101 *ori*, Km$^r$, *rne*-E429G under $P_{BAD}$ | This study |
| pET3a | pBR322 *ori*, Amp$^r$ | Novagen |
| pET3a-RNA $I_{-5}$ | pBR322 *ori*, Amp$^r$, RNA $I_{-5}$ | This study |

*Amp$^r$* ampicillin resistance, *Km$^r$* kanamycin resistance, *$P_{BAD}$* araBAD promoter

**Table 2** Oligonucleotides used in this study

| Oligonucleotides | Sequences (5′–3′) |
|---|---|
| *For gene cloning* | |
| RNA I-5del (F) | GGAAAGAACATGTGAGCAAA |
| RNA I-5del-M (R) | GCAGAGCGCAGATACCAAATGCTTCTAGTGTAGCCGTAG |
| RNA I-5del-M (F) | ACTACGGCTACACTAGAAGGATTTGGTATCTGCGCTCTGC |
| RNA I-5del (R) | ACGATGCCTGCAGCAATGGC |
| *For Northern blot* | |
| RNA I loop 3 probe (+13 and +38) | ACCGCTACCAGCGGTGGTTTGTTTGC |
| 5S rRNA probe (+41 and +60) | ACTACCATCGGCGCTACGGC |
| M1 RNA probe (+119 and +138) | GCTCTCTGTTGCACTGGTCG |
| *For primer extension* | |
| RNA I-PE (+16 and +44) | GCTACCAGCGGTGGTTTGTTTGCCGGATC |

incubated for 10 h in a shaking incubator at 240 rpm. The $OD_{600}$ values of the bacterial culture were measured using a Biophotometer D30 (Eppendorf) every 60 min for 10 h continuously. Three or more replicates were carried out for all the growth-curve measurements.

## Western Blotting Analysis

Western blotting analysis was performed as described previously (Moore et al., 2021). KSL2000-derived strains were grown to an $OD_{600}$ value of 0.7 and harvested. Membranes were blotted with primary antibodies against His (1:1000) and S1 (1:10,000) overnight at 4 °C. The blots were then incubated with the secondary antibodies, anti-mouse IgG (1:10,000) for anti-His and anti-rabbit IgG (1:10,000) for anti-S1, for 4 h.

## Protein Stability Analysis

KSL2000-derived cells were grown in LB medium containing 100 μg/ml kanamycin, 5 μg/ml tetracycline, and 5 μg/ml chloramphenicol and supplemented with 0.1% L-arabinose at 37 °C at an $OD_{600}$ of 0.8. The cells were harvested at 5000 rpm for 10 min at 4 °C. The cell pellets were resuspended in LB medium containing 100 μg/ml kanamycin, 5 μg/ml tetracycline, and 5 μg/ml chloramphenicol and further incubated at 37 °C for 10 min. Spectinomycin was then added at a final concentration of 1 mg/ml (time = 0). Samples were collected at the indicated time points and subjected to SDS-PAGE and western blotting analyses.

## Northern Blotting Analysis

Northern blotting analysis was performed as described previously (Lee et al., 2002, 2021a, 2021b, 2021c). In brief, total RNA was extracted from cultures of KSL2000-derived cells grown at 37 °C in LB media containing 100 μg/ml kanamycin, 5 μg/ml tetracycline, and 5 μg/ml chloramphenicol and supplemented with 0.1% L-arabinose to an $OD_{600}$ of 0.8 using hot phenol methods. 15 μg of total RNA was analyzed on a 12% polyacrylamide gel containing 8 M urea. Blots were hybridized using specific probes for the RNA I. The northern blot membranes were then stripped and reprobed with a radiolabelled probe specific for the 5S rRNA or M1 RNA. RNA I loop 3 probes was used to probe RNA I, while 5S rRNA and M1 probes were used to probe 5S rRNA and M1 RNA, respectively. Synthetic RNA I and the in vitro cleavage product of RNA I by RNase E were used as the positive controls.

## Measurement of ColE1-Type Plasmid Copy Number

The measurement of plasmid copy number has been described previously (Lee et al., 2009; Park et al., 2017; Yeom & Lee, 2006; Yeom et al., 2008). KSL2000-derived cells harboring pET3a or pET3a-RNA $I_{-5}$ were grown in LB medium with the appropriate antibiotics (100 μg/ml ampicillin, 100 μg/ml kanamycin, 5 μg/ml tetracycline, and 5 μg/ml chloramphenicol) and 0.1% L-arabinose at 37 °C to an $OD_{600}$ of 1.0. Isolated plasmids were digested with the restriction enzyme, EcoRI, which has a unique cleavage site in all plasmids. Plasmid copy numbers were calculated relative to a concurrently present pSC101 derivative (pBAD-RNE, pBAD-RNE-Q36R, and pBAD-RNE-E429G), which was replicated independent of Rne, by measuring the molar ratio of the ColE1-type plasmid (pET3a or pET3a-RNA $I_{-5}$) to that of the pBAD-RNE plasmid. DNA quantification was performed using the Quantity One software (Bio-Rad).

## Primer Extension

Total RNA was isolated as described previously (Choi et al., 2022; Lin-Chao & Cohen, 1991). Primer extension analysis was performed as described previously (Song et al., 2019). The 5′-end of the oligonucleotide primer (RNAI-PE) was radiolabeled with [$\gamma$-$^{32}$P] ATP (3000 Ci/mmol)

(PerkinElmer) and T4 polynucleotide kinase (New England Biolabs). The extended fragments were analyzed on a 10% polyacrylamide gel containing 8 M urea. Sequencing ladders were generated using dideoxy NTP and pET3a (Jena Bioscience).

### Quantification and Statistical Analyses

The statistical details for all the experiments are included in the figure legends. Statistical analyses were performed as described previously (Lee et al., 2019; Veena et al., 2021).

## Results

### Analysis of the Stability of Wild-Type (WT) and Hyperactive RNase E Proteins

To determine whether the presence of hyperactive mutations affected the RNase E stability, S30 extracts were prepared from KSL2000 (Rne-WT) strain and its derivatives expressing hyperactive RNase E variants (KSL2000-Q36R and KSL2000-E429G). These strains have a deletion in the chromosomal *rne* gene, which was substituted with the plasmid-borne *rne* gene under the control of an arabinose-inducible promoter (pBAD-RNE, pBAD-RNE-Q36R, and pBAD-RNE-E429G) (Lee et al., 2002). The growth rates and yields of KSL2000-Q36R and KSL2000-E429G strains were moderately lower than those of the KSL2000 strain (Fig. 1A). However, the expression levels of the Rne proteins were not significantly altered in any of the strains used in these experiments (Fig. 1B).

Next, we measured the RNase E stability in these strains. KSL2000 and its derivatives were transferred to a fresh medium without arabinose to repress *rne* gene expression and spectinomycin (1 mg/ml) was added to inhibit protein synthesis. Then, cells were harvested at different time intervals, and Rne protein levels were measured via western blotting. As shown in Fig. 2, the stability of Rne variants was similar to that of Rne-WT. The findings suggest that these mutations do not alter the stability of Rne.

### Effect of the Hyperactive RNase E Mutation on the Cleavage Activity of RNA I In vivo

Next, we investigated whether two different hyperactive RNase E mutations affected the cleavage specificity of the enzyme. The cleavage specificity of the hyperactive RNase E variants was analyzed via northern blotting using RNA I, a well-characterized RNase E substrate (Fig. 3). The major RNase E cleavage site in RNA I is located between the 5th and 6th nucleotides from the 5′-end of RNA I, generating RNA $I_{-5}$ (Masukata & Tomizawa, 1984; Tamm & Polisky, 1985). Synthetic RNA I and the in vitro cleavage product of RNA I by RNase E were used as the positive controls. The results showed that KSL2000 cells produced only RNA $I_{-5}$ as an RNA I cleavage product (lane 2 in Fig. 3A), whereas KSL2000 cells expressing Rne-Q36R or Rne-E429G produced other minor products along with RNA $I_{-5}$ (lanes 4 and 5 in Fig. 3A). The abundance of RNA $I_{-5}$ in KSL2000-Q36R and KSL2000-E429G cells was higher than that in KSL2000 cells. These results indicate that both Rne-Q36R and Rne-E429G proteins have hyperactive ribonucleolytic activity and relaxed cleavage specificity for RNA I. No other

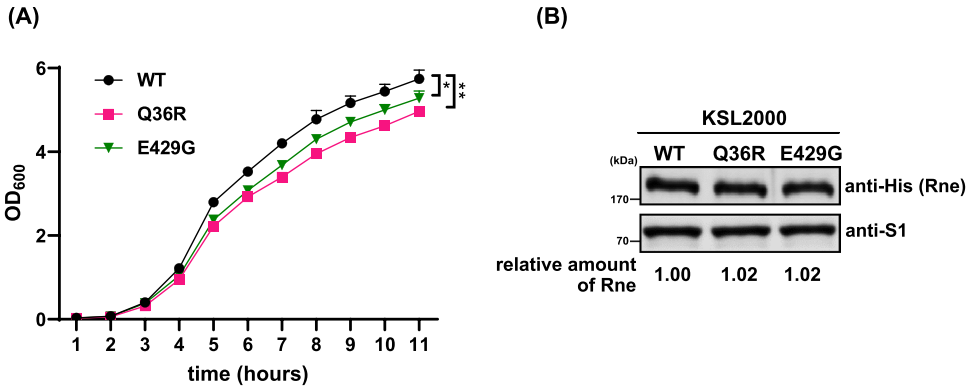


**Fig. 1** Effects of the expression levels of hyperactive RNase E variants on the growth of *E. coli*. **A** Growth characteristics of cells expressing Rne mutants. KSL2000 cells harboring pBAD-RNE, pBAD-RNE-Q36R, or pBAD-RNE-E429G were evaluated in the LB medium supplemented with 0.1% L-arabinose, 100 μg/ml kanamycin, 5 μg/ml tetracycline, and 5 μg/ml chloramphenicol, and the growth was monitored by measuring the optical density at 600 nm ($OD_{600}$) at indicated time intervals. The data are presented as the mean ± SEM from three independent experiments. Asterisks indicate the statistically significant differences (*$p < 0.05$, **$p < 0.01$). **B** Cells were harvested in log phase ($OD_{600} = 0.7$) to obtain total protein samples for western blotting analysis. The membrane was probed with an anti-His monoclonal antibody. S1 protein was used as an internal standard. Relative abundance of Rne protein was quantified by setting the amount of Rne-WT to 1

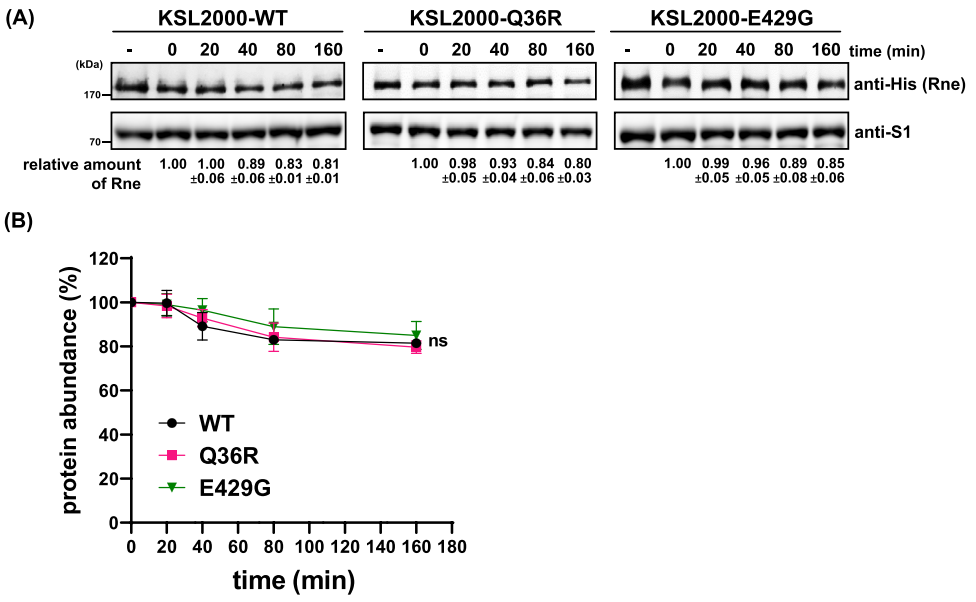


**Fig. 2** Analysis of the stability of Rne-WT and hyperactive Rne proteins. **A** Representative western blots showing the decay of Rne proteins. Cells were grown in LB medium containing 0.1% L-arabinose. The cultures were grown to $OD_{600} = 0.8$, transferred to a fresh medium, and protein synthesis was blocked by adding spectinomycin. Samples were taken at the indicated time points and subjected to western blotting analysis. **B** Decay rates of Rne proteins. Graph shows the percentage of remaining Rne after treatment with spectinomycin. The data are presented as the mean ± SEM from three independent experiments. Asterisks indicate the statistically significant differences (*ns* not significant)

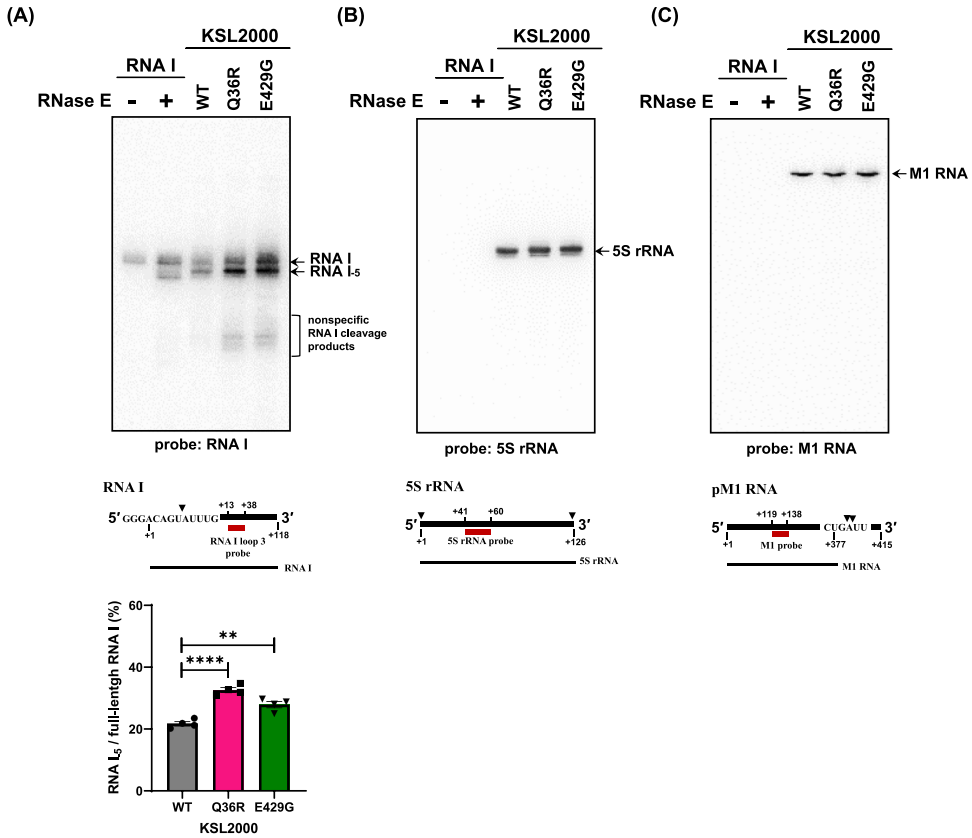


**Fig. 3** Ribonucleolytic activity of hyperactive RNase E variants on RNase E substrates. Northern blotting analysis of RNA I, 5S rRNA and M1 RNA. Total RNA (15 µg) was analyzed on a 12% polyacrylamide gel containing 8 M urea. Percentage of RNA $I_{-5}$ compared to full-length RNA I are shown. The data are presented as the mean ± SEM from three independent experiments. Asterisks indicate the statistically significant differences (**$p < 0.01$, ****$p < 0.0001$). Blots were hybridized using specific probes **A** for the RNA I. The northern blot membranes were then stripped and reprobed with a radiolabelled probe specific **B** for the 5S rRNA or **C** M1 RNA. Synthetic RNA I and the in vitro cleavage product of RNA I by RNase E were used as the positive controls. Specific binding sites for each probe are shown under the gel

cleavage products were observed with 5S rRNA and M1 RNA.

## Effect of the Hyperactive Mutation of RNase E on the Replication of ColE1-Type Plasmid

Since RNase E regulates the copy number of ColE1-type plasmids by cleaving RNA I, plasmid copy number analysis is used to assess the RNase E activity in vivo (Go et al., 2011; Lin-Chao et al., 1994). We used this analysis to assess the in vivo ribonucleolytic activity of the hyperactive RNase E variants. KSL2000-Q36R and KSL2000-E429G harboring a ColE-1 type plasmid (pET3a) showed 2- and 1.7-fold higher plasmid copy numbers, respectively, compared to that of KSL2000 harboring pET3a, as previously reported (Fig. 4) (Go et al., 2011; Moore et al., 2021). In these experiments, the plasmid copy numbers of pET3a were calculated relative to a concurrently present pSC101 derivative (pBAD-RNE, pBAD-RNE-Q36R, and pBAD-RNE-E429G), which replicated independent of Rne, by measuring the molar ratio of the ColE1-type plasmid (pET3a) to that of the pBAD-RNE plasmid. These results show that the hyperactive RNase E variants cleave RNA I with a higher efficiency than WT RNase E, as previously reported (Go et al., 2011; Moore et al., 2021).

To determine whether the non-specific cleavage activity of the hyperactive RNase E variants affected the plasmid copy number of pET3a, we constructed an RNA $I_{-5}$ expression system by deleting the first five nucleotides from the RNA I-coding region in pET3a, resulting in pET3a-RNA $I_{-5}$. The plasmid copy numbers of pET3a-RNA $I_{-5}$ were calculated relative to a concurrently present pSC101 derivative (pBAD-RNE, pBAD-RNE-Q36R, and pBAD-RNE-E429G). Cells expressing WT RNase E showed an approximately twofold increase in the copy number of pET3a-RNA $I_{-5}$ relative to that of pET3a in cells expressing WT RNase E (Fig. 4). Analogous results were obtained when hyperactive RNase E variants were expressed with pET3a-RNA $I_{-5}$. These results indicate that the in vivo function of RNA I as an antisense regulator is lost when five nucleotides are removed from the 5′-end of RNA I.

## Identification of Cryptic RNase E Cleavage Sites in RNA I In vivo

To characterize the cryptic RNase E cleavage sites generated by the relaxed cleavage specificity of hyperactive RNase E variants, we performed primer extension analysis on RNA I and its derivative, RNA $I_{-5}$, using total RNA extracted from the six strains shown in Fig. 4. For these experiments, a 5′-end $^{32}$P-labeled primer (RNA I-PE) was

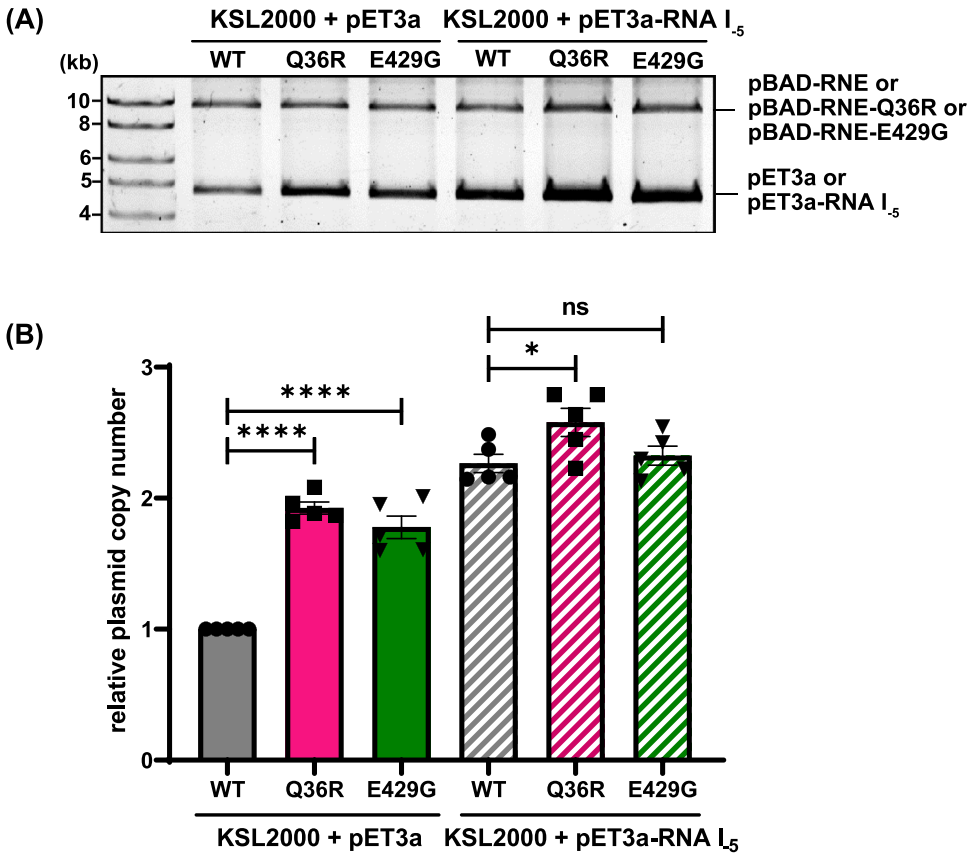


**Fig. 4** Effects of the expression levels of RNA $I_{-5}$ and hyperactive RNase E variants on the copy number of ColE-1 type plasmid. Plasmids were purified from KSL2000 (Rne-WT, Rne-Q36R, and Rne-E429G) cells harboring pET3a or pET3a-RNA $I_{-5}$, and digested with EcoRI. Plasmid copy numbers were calculated relative to the concurrently present pSC101 derivatives (pBAD-RNE, pBAD-RNE-Q36R, and pBAD-RNE-E429G) by measuring the molar ratio of the ColE1-type plasmid (pET3a or pET3a-RNA $I_{-5}$) to the pBAD-RNE plasmid, and are shown at the bottom of the gel. Quantified data are presented as the mean ± SEM of three independent experiments. Asterisks indicate the statistically significant differences (*$p < 0.05$, ****$p < 0.0001$; *ns* not significant)

designed to bind near the 3′-end of RNA I (from position + 16 to + 44) and extended using AMV reverse transcriptase. When hyperactive RNase E variants and RNA I were expressed, 11 distinct cDNA bands (blue arrows) were detected, which were not found in samples from KSL2000 cells harboring pET3a (Fig. 5). However, these cDNA bands were detected when RNA $I_{-5}$ was expressed in all strains, regardless of the RNase E type (Fig. 5). In addition, three additional cDNA bands (orange arrows) were detected in cells expressing RNA $I_{-5}$ (Fig. 5). Most of the cleavage sites deduced from the 11 cDNA bands (blue arrows) were located in the consensus motif of RNase E (Chao et al., 2017) or in the AU-rich region. In contrast, all sequences in the orange arrow bands were present in the loops. It is possible that hyperactive RNase E can cleave non-specifically at sites similar to RNase E cleavage motifs, which can also be recognized by WT RNase E when the major RNase E cleavage site is removed. We also observed that steady-state levels of RNA $I_{-5}$ increased by approximately two-fold in cells expressing RNA $I_{-5}$ compared to those in cells expressing RNA I (Fig. 5). These results indicate that RNA $I_{-5}$ does not function as efficiently as RNA I as an antisense RNA, which has been suggested previously using in vitro binding assays (Tamm & Polisky, 1985; Tomizawa, 1984).

## Discussion

Rne-Q36R and Rne-E429G variants show enhanced catalytic activity by decreasing the non-competitive inhibition of RNA substrates or enhancing the multimerization of RNase E, respectively (Go et al., 2011; Moore et al., 2021). In this study, we investigated the effects of hyperactive mutations on the cleavage specificity of the target RNA substrate, RNA I. When the growth curves of the strains expressing WT RNase E or hyperactive RNase E variants were measured, Q36R and E429G mutations resulted in lower growth rates and yields compared to the WT (Fig. 1A). Since RNase E is involved in the processing and degradation of various RNAs and predominantly regulates the transcripts encoding proteins in energy production pathways (Bernstein et al., 2002; Lee et al., 2002), it is possible that the hyperactivity of RNase E altered the abundance of the RNA substrates, leading to changes in gene expression and consequently affecting the cellular growth.

RNase E is an endoribonuclease that cleaves the AU-rich region of single-stranded RNA (Huang et al., 1998; McDowall et al., 1994). Presence of uridine 2 nt downstream in a single-stranded segment is the key recognition structure favored by RNase E catalysis (Chao et al., 2017). The hyperactive RNase E variants appeared to recognize uridine or cytosine 2 nt downstream of the cleavage site ($U_{+2}$, $C_{+2}$)

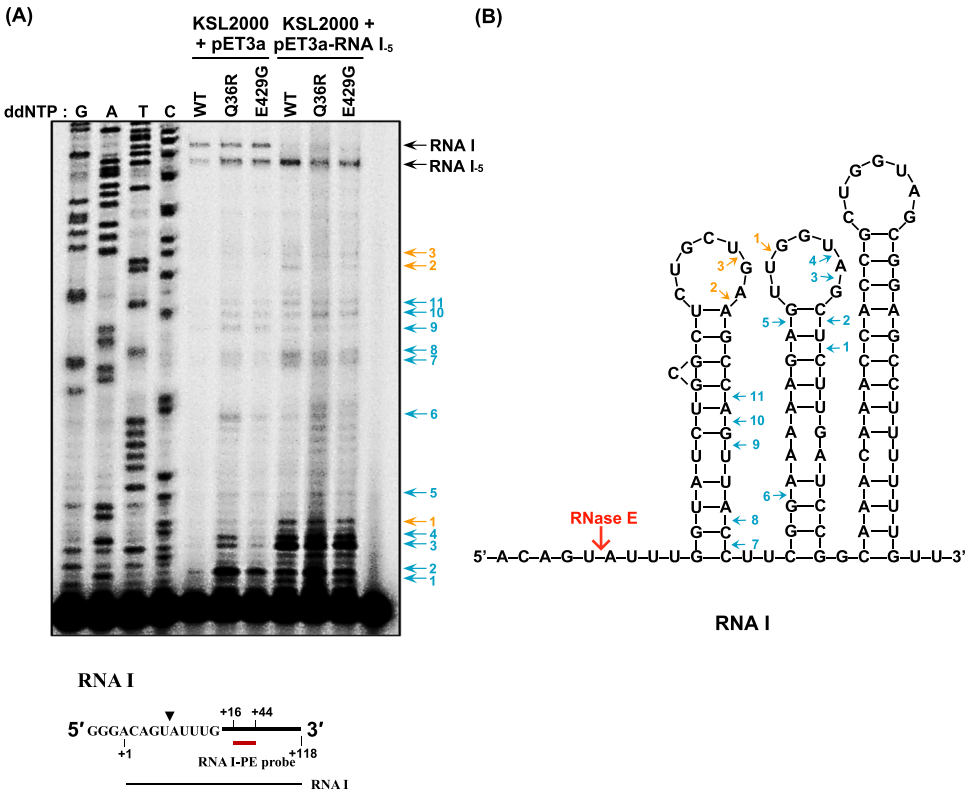


**Fig. 5** Primer extension analysis of RNase E cleavage sites in RNA I and RNA $I_{-5}$. **A** Total RNA was isolated from KSL2000, KSL2000-Q36R, and KSL2000-E429G cells harboring pET3a or pET3a-RNA $I_{-5}$ and hybridized with the 5′-end $^{32}$P-labeled primer (RNA I-PE). Synthesized cDNA products were separated on a 10% polyacrylamide gel containing 8 M urea. Sequencing ladders were synthesized using the same primer used for cDNA synthesis with pET3a as a template. **B** RNase E cleavage sites in RNA I. Major cleavage sites of RNase E (red and blue arrows) and other cryptic sites identified in **A** are indicated in RNA I (orange arrows). Specific binding sites for the probe are shown under the gel

(Fig. 5), as has been previously suggested (Chao et al., 2017). A similar cleavage specificity was observed when RNA $I_{-5}$ was expressed. Based on our results, it is tempting to speculate that the cleavage flexibility of RNase E, proposed in the study of the $U_{+2}$ Ruler-and-Cut mechanism by Chao et al. (2017), was maximized due to these hyperactive mutations, resulting in the increased non-specific cleavage of RNA I. The higher cleavage flexibility of two hyperactive RNase E variants might stem from their higher cleavage rates on both major and cryptic sites for the following reasons. First, these variants do not share the mechanism for increased ribonucleolytic activity (Go et al., 2011; Moore et al., 2021; Shin et al., 2008). Second, both mutations do not enhance substrate RNA binding (Go et al., 2011; Moore et al., 2021; Shin et al., 2008). Thus, perhaps, these variants scan cleavage sites from the 5′-end of RNA I and cleave at cryptic sites before scanning further downstream or being released from the substrate (Richards & Belasco, 2021). Further studies are needed to characterize the mechanism underlying the increased cleavage flexibility of these variants.

In addition, our data indicated that hyperactive mutations in RNase E resulted in the non-specific cleavage of RNA I, regardless of the presence of the RNase E major cleavage site on RNA I. When the major RNase E cleavage site was removed, WT RNase E cleaved the same sites on target RNA I as hyperactive RNase E variants. Three additional cleavage products were detected when RNA $I_{-5}$ was expressed. These results may stem from the unstable binding of RNA $I_{-5}$ to RNA II, which can alter the stability and structure of RNA $I_{-5}$.

RNA $I_{-5}$ expression resulted in an approximately twofold increase in the copy number of the ColE-1 type plasmid and the steady-state levels of RNA $I_{-5}$ compared to those in cells expressing RNA I (Figs. 4 and 5). These results indicate that RNA $I_{-5}$ does not efficiently function as an antisense RNA, even though RNA $I_{-5}$ is stabilized when expressed in a triphosphorylated form, which protects RNA from ribonuclease attack. These results are consistent with those of a previous study that suggested the importance of five nucleotides at the 5′-end of RNA I for the efficient formation of a complex between RNA I and RNA II (Tamm & Polisky, 1985; Tomizawa, 1984). Relaxed substrate specificity (star activity) can be easily detected under nonoptimal conditions for many restriction enzymes that cleave double-stranded DNAs in a sequence-specific manner (Nasri & Thomas, 1986; Robinson & Sligar, 1995, 1998). Since the relaxed specificities are intrinsic properties of endonucleases, it is assumed that organisms have evolved to possess endonucleases with lower off-target rates. In conclusion, our study suggests that hyperactive RNase E variants are not evolutionarily selected probably because of relaxed cleavage specificity and reveal a previously unidentified property of RNA $I_{-5}$ in vivo.

**Acknowledgements** This research was supported by the National Research Foundation of Korea [NRF-2021R1A2C3008934 to K. L. and NRF-2021R1I1A1A01056162 to J-H. Y]. This research was also supported by the Chung-Ang University Graduate Research Scholarship in 2021.

**Data availability** All data generated or analysed in this study are included in the published article.

## Declarations

**Conflict of interest** The authors declare that they have no conflicts of interest.

## References

Arraiano, C. M., Andrade, J. M., Domingues, S., Guinote, I. B., Malecki, M., Matos, R. G., Moreira, R. N., Pobre, V., Reis, F. P., Saramago, M., Silva, I. J., & Viegas, S. C. (2010). The critical role of RNA processing and degradation in the control of gene expression. *FEMS Microbiology Reviews, 34*, 883–923.

Bandyra, K. J., Wandzik, J. M., & Luisi, B. F. (2018). Substrate recognition and autoinhibition in the central ribonuclease RNase E. *Molecular Cell, 72*(275–285), e274.

Bernstein, J. A., Khodursky, A. B., Lin, P. H., Lin-Chao, S., & Cohen, S. N. (2002). Global analysis of mRNA decay and abundance in *Escherichia coli* at single-gene resolution using two-color fluorescent DNA microarrays. *Proceedings of the National Academy of Sciences of the United States of America, 99*, 9697–9702.

Callaghan, A. J., Marcaida, M. J., Stead, J. A., McDowall, K. J., Scott, W. G., & Luisi, B. F. (2005). Structure of *Escherichia coli* RNase E catalytic domain and implications for RNA turnover. *Nature, 437*, 1187–1191.

Chao, Y., Li, L., Girodat, D., Forstner, K. U., Said, N., Corcoran, C., Smiga, M., Papenfort, K., Reinhardt, R., Wieden, H. J., Luisi, B. F., & Vogel, J. (2017). In vivo cleavage map illuminates the central role of RNase E in coding and non-coding RNA pathways. *Molecular Cell, 65*, 39–51.

Choi, Y., Joo, M., Song, W., Lee, M., Hyeon, H., Kim, H. L., Yeom, J. H., Lee, K., & Shin, E. (2022). Transcript-specific selective translation by specialized ribosomes bearing genome-encoded heterogeneous rRNAs in *V. vulnificus* CMCP6. *Journal of Microbiology, 60*, 1162–1167.

Cohen, S. N. (1995). Surprises at the 3' end of prokaryotic RNA. *Cell, 80*, 829–832.

Feng, Y., Vickers, T. A., & Cohen, S. N. (2002). The catalytic domain of RNase E shows inherent 3' to 5' directionality in cleavage site selection. *Proceedings of the National Academy of Sciences of the United States of America, 99*, 14746–14751.

Gao, J., Lee, K., Zhao, M., Qiu, J., Zhan, X., Saxena, A., Moore, C. J., Cohen, S. N., & Georgiou, G. (2006). Differential modulation of *E. coli* mRNA abundance by inhibitory proteins that alter the composition of the degradosome. *Molecular Microbiology, 61*, 394–406.

Ghora, B. K., & Apirion, D. (1978). Structural analysis and in vitro processing to p5 rRNA of a 9S RNA molecule isolated from an rne mutant of *E. coli*. *Cell, 15*, 1055–1066.

Go, H., Moore, C. J., Lee, M., Shin, E., Jeon, C. O., Cha, C. J., Han, S. H., Kim, S. J., Lee, S. W., Lee, Y., Ha, N. C., Kim, Y. H., Cohen, S. N., & Lee, K. (2011). Upregulation of RNAse E activity by mutation of a site that uncompetitively interferes with RNA binding. *RNA Biology, 8*, 1022–1034.

Goldblum, K., & Apirion, D. (1981). Inactivation of the ribonucleic acid-processing enzyme ribonuclease E blocks cell division. *Journal of Bacteriology, 146*, 128–132.

Gurevitz, M., & Apirion, D. (1983). Interplay among processing and degradative enzymes and a precursor ribonucleic acid in the selective maturation and maintenance of ribonucleic acid molecules. *Biochemistry, 22*, 4000–4005.

Gurevitz, M., Jain, S. K., & Apirion, D. (1983). Identification of a precursor molecular for the RNA moiety of the processing enzyme RNase P. *Proceedings of the National Academy of Sciences of the United States of America, 80*, 4450–4454.

Hagege, J. M., & Cohen, S. N. (1997). A developmentally regulated streptomyces endoribonuclease resembles ribonuclease e of *Escherichia coli*. *Molecular Microbiology, 25*, 1077–1090.

Huang, H., Liao, J., & Cohen, S. N. (1998). Poly(A)- and poly(U)-specific RNA 3' tail shortening by *E. coli* ribonuclease E. *Nature, 391*, 99–102.

Jain, C., & Belasco, J. G. (1995). RNase E autoregulates its synthesis by controlling the degradation rate of its own mRNA in *Escherichia coli*: Unusual sensitivity of the rne transcript to RNase E activity. *Genes & Development, 9*, 84–96.

Jiang, X., & Belasco, J. G. (2004). Catalytic activation of multimeric RNase E and RNase G by 5'-monophosphorylated RNA. *Proceedings of the National Academy of Sciences of the United States of America, 101*, 9211–9216.

Kido, M., Yamanaka, K., Mitani, T., Niki, H., Ogura, T., & Hiraga, S. (1996). RNase E polypeptides lacking a carboxyl-terminal half suppress a mukB mutation in *Escherichia coli*. *Journal of Bacteriology, 178*, 3917–3925.

Kim, S., Kim, H., Park, I., & Lee, Y. (1996). Mutational analysis of RNA structures and sequences postulated to affect 3' processing of m1 RNA, the RNA component of *Escherichia coli* RNase P. *Journal of Biological Chemistry, 271*, 19330–19337.

Lee, K., Bernstein, J. A., & Cohen, S. N. (2002). RNase G complementation of rne null mutation identifies functional interrelationships with RNase E in *Escherichia coli*. *Molecular Microbiology, 43*, 1445–1456.

Lee, K., & Cohen, S. N. (2003). A *Streptomyces coelicolor* functional orthologue of *Escherichia coli* RNase E shows shuffling of catalytic and PNPase-binding domains. *Molecular Microbiology, 48*, 349–360.

Lee, J., Lee, D. H., Jeon, C. O., & Lee, K. (2019). RNase G controls tpiA mRNA abundance in response to oxygen availability in *Escherichia coli*. *Journal of Microbiology, 57*, 910–917.

Lee, J., Lee, M., & Lee, K. (2021a). Trans-acting regulators of ribonuclease activity. *Journal of Microbiology*, *59*, 341–359.

Lee, M., Ryu, M., Joo, M., Seo, Y. J., Lee, J., Kim, H. M., Shin, E., Yeom, J. H., Kim, Y. H., Bae, J., & Lee, K. (2021b). Endoribonuclease-mediated control of hns mRNA stability constitutes a key regulatory pathway for salmonella typhimurium pathogenicity island 1 expression. *PLoS Pathogens, 17*, e1009263.

Lee, J., Shin, E., Park, J., Lee, M., & Lee, K. (2021c). Regulator of ribonuclease activity modulates the pathogenicity of *Vibrio vulnificus*. *Journal of Microbiology, 59*, 1133–1141.

Lee, J., Shin, E., Yeom, J. H., Park, J., Kim, S., Lee, M., & Lee, K. (2022). Regulator of RNase E activity modulates the pathogenicity of salmonella typhimurium. *Microbial Pathogenesis, 165*, 105460.

Lee, M., Yeom, J. H., Sim, S. H., Ahn, S., & Lee, K. (2009). Effects of *Escherichia coli* rRAA orthologs of *Vibrio vulnificus* on the ribonucleolytic activity of RNase E in vivo. *Current Microbiology, 58*, 349–353.

Li, Z., & Deutscher, M. P. (2002). RNase E plays an essential role in the maturation of *Escherichia coli* tRNA precursors. *RNA, 8*, 97–109.

Li, Z., Pandit, S., & Deutscher, M. P. (1999). RNase G (CafA protein) and RNase E are both required for the 5' maturation of 16S ribosomal RNA. *EMBO Journal, 18*, 2878–2885.

Lin-Chao, S., & Cohen, S. N. (1991). The rate of processing and degradation of antisense RNAI regulates the replication of ColE1-type plasmids in vivo. *Cell, 65*, 1233–1242.

Lin-Chao, S., Wong, T. T., McDowall, K. J., & Cohen, S. N. (1994). Effects of nucleotide sequence on the specificity of rne-dependent and RNase E-mediated cleavages of RNA I encoded by the pBR322 plasmid. *Journal of Biological Chemistry, 269*, 10797–10803.

Mackie, G. A. (1998). Ribonuclease E is a 5'-end-dependent endonuclease. *Nature, 395*, 720–723.

Masukata, H., & Tomizawa, J. (1984). Effects of point mutations on formation and structure of the RNA primer for ColE1 DNA replication. *Cell, 36*, 513–522.

McDowall, K. J., & Cohen, S. N. (1996). The n-terminal domain of the rne gene product has RNase E activity and is non-overlapping with the arginine-rich RNA-binding site. *Journal of Molecular Biology, 255*, 349–355.

McDowall, K. J., Kaberdin, V. R., Wu, S. W., Cohen, S. N., & Lin-Chao, S. (1995). Site-specific RNase E cleavage of oligonucleotides and inhibition by stem-loops. *Nature, 374*, 287–290.

McDowall, K. J., Lin-Chao, S., & Cohen, S. N. (1994). A+U content rather than a particular nucleotide order determines the specificity of RNase E cleavage. *Journal of Biological Chemistry, 269*, 10790–10796.

Moore, C. J., Go, H., Shin, E., Ha, H. J., Song, S., Ha, N. C., Kim, Y. H., Cohen, S. N., & Lee, K. (2021). Substrate-dependent effects of quaternary structure on RNase E activity. *Genes & Development, 35*, 286–299.

Nasri, M., & Thomas, D. (1986). Relaxation of recognition sequence of specific endonuclease HindIII. *Nucleic Acids Research, 14*, 811–821.

Park, N., Heo, J., Song, S., Jo, I., Lee, K., & Ha, N. C. (2017). Crystal structure of *Streptomyces coelicolor* RraAS2, an unusual member of the RNase E inhibitor RraA protein family. *Journal of Microbiology, 55*, 388–395.

Richards, J., & Belasco, J. G. (2021). Widespread protection of RNA cleavage sites by a riboswitch aptamer that folds as a compact obstacle to scanning by RNase E. *Molecular Cell, 81*(127–138), e124.

Robinson, C. R., & Sligar, S. G. (1995). Heterogeneity in molecular recognition by restriction endonucleases: osmotic and hydrostatic pressure effects on BamHI, Pvu II, and EcoRV specificity. *Proceedings of the National Academy of Sciences of the United States of America, 92*, 3444–3448.

Robinson, C. R., & Sligar, S. G. (1998). Changes in solvation during DNA binding and cleavage are critical to altered specificity of the EcoRI endonuclease. *Proceedings of the National Academy of Sciences of the United States of America, 95*, 2186–2191.

Shin, E., Go, H., Yeom, J. H., Won, M., Bae, J., Han, S. H., Han, K., Lee, Y., Ha, N. C., Moore, C. J., Sohlberg, B., Cohen, S. N., & Lee, K. (2008). Identification of amino acid residues in the catalytic domain of RNase E essential for survival of *Escherichia coli*: functional analysis of DNase I subdomain. *Genetics, 179*, 1871–1879.

Singh, D., Chang, S. J., Lin, P. H., Averina, O. V., Kaberdin, V. R., & Lin-Chao, S. (2009). Regulation of ribonuclease e activity by the L4 ribosomal protein of *Escherichia coli*. *Proceedings of the National Academy of Sciences of the United States of America, 106*, 864–869.

Song, W., Joo, M., Yeom, J. H., Shin, E., Lee, M., Choi, H. K., Hwang, J., Kim, Y. I., Seo, R., Lee, J. E., Moore, C. J., Kim, Y. H., Eyun, S. I., Hahn, Y., Bae, J., & Lee, K. (2019). Divergent rRNas as

regulators of gene expression at the ribosome level. *Nature Microbiology, 4*, 515–526.

Tamm, J., & Polisky, B. (1985). Characterization of the ColE1 primer-RNA1 complex: Analysis of a domain of ColE1 RNA1 necessary for its interaction with primer RNA. *Proceedings of the National Academy of Sciences of the United States of America, 82*, 2257–2261.

Tomizawa, J. (1984). Control of ColE1 plasmid replication: The process of binding of RNA I to the primer transcript. *Cell, 38*, 861–870.

Updegrove, T. B., Kouse, A. B., Bandyra, K. J., & Storz, G. (2019). Stem-loops direct precise processing of 3' UTR-derived small RNA MicL. *Nucleic Acids Research, 47*, 1482–1492.

Veena, H., Gowda, S. K., Achur, R. N., & Thippeswamy, N. B. (2021). Molecular mechanism of *Escherichia coli* H10407 induced diarrhoea and its control through immunomodulatory action of bioactives from *Simarouba amara* (Aubl.). *Journal of Microbiology, 59*, 435–447.

Xu, F., Lin-Chao, S., & Cohen, S. N. (1993). The *Escherichia coli* pcnB gene promotes adenylylation of antisense RNAI of ColE1-type plasmids in vivo and degradation of RNAI decay intermediates. *Proceedings of the National Academy of Sciences of the United States of America, 90*, 6756–6760.

Yeom, J. H., & Lee, K. (2006). RraA rescues *Escherichia coli* cells over-producing RNase E from growth arrest by modulating the ribonucleolytic activity. *Biochemical and Biophysical Research Communications, 345*, 1372–1376.

Yeom, J. H., Shin, E., Go, H., Sim, S. H., Seong, M. J., & Lee, K. (2008). Functional implications of the conserved action of regulators of ribonuclease activity. *Journal of Microbiology and Biotechnology, 18*, 1353–1356.